EUROPEAN FUSION DEVELOPMENT AGREEMENT

EFDA–JET–CP(01)06-03

M. Becoulet, V. Parail, G. Huysmans, S. Sharapov, P.J. Lomas, G. Saibene[2], R. Sartori[2], A. Loarte[2], G.F Matthews, W. Suttrop[3], J. Stober[3], A. Kallenbach[3], E. Joffrin[1], Y. Sarazin[1], X. Litaudon[1], A. Becoulet[1], Ph. Ghendrih[1] and JET-EFDA contributors

ELMs Behaviour and Edge Plasma Stability in JET

ELMs Behaviour and Edge Plasma Stability in JET

M. Becoulet[1], V. Parail, G. Huysman[1], S. Sharapov, P.J. Lomas, G. Saibene[2], R. Sartori[2], A. Loarte[2], G.F Matthews, W. Suttrop[3], J. Stober[3], A. Kallenbach[3], E. Joffrin[1], Y. Sarazin[1], X. Litaudon[1], A. Becoulet[1], Ph. Ghendrih[1] and JET-EFDA contributors

EURATOM/UKAEA Fusion Association, Culham Science Centre, Abingdon, Oxfordshire, OX14 3DB, UK.

[1]Association Euratom-CEA, CEA Cadarache, F-13108 St Paul lez Durance, Cedex, France.

[2]EFDA Close Support Unit, Garching, Max-Planck-Institut für Plasmaphysik, Boltzmannstraße 2, Garching, Germany.

[3]Association Euratom-IPP, Max-Planck-Institut für Plasmaphysik, Boltzmannstraße 2, Garching, Germany.

**See Annex of J. Pamela et al., "Overview of Recent JET Results and Future Perspectives", Fusion Energy 2000 (Proc. 18th Int. Conf. Sorrento, 2000), IAEA, Vienna (2001).*

Preprint of Paper to be submitted for publication in Proceedings of the H-mode Workshop, (NIFS, Toki, Japan 4-7 September 2001)

ABSTRACT.

This paper presents recent experimental results and plasma edge stability studies of ELMs, for both H-mode and Optimised Shear (OS) plasmas in JET. The high triangularity (δ~0.5) ELMy H-mode experiments in JET are presented in the first part of the paper. These plasmas achieved simultaneously high confinement (H_{97}=1) and high density (~0.9n_{GR}). In this scenario, high pedestal pressure and type I ELMs are observed up to the highest density (~1.1n_{GR}). Moreover, at high pedestal density, an anomalous decrease of type I ELMs frequency and energy losses per ELM is observed, associated to an increased MHD signal between type I ELMs with mainly n=-8 toroidal number, and frequency in the range of <30Hz kHz. This behaviour was associated with type II-like ELMs activity by analogy with ASDEX–U observations. Type II-like ELMs were observed in JET at rather low q_{95}~3, compared to other machines. The coupled JETTO-MISHKA transport and MHD stability analysis for high triangularity, high density scenarios confirmed a possible access to the second stability zone for the ballooning modes and stability for peeling modes at the same time. The second part of the paper is devoted to the experimental comparative study of the transition from Type I to Type III ELMs , carried out in the same plasma configurations for standard ELMy H-modes and OS plasmas. The type III to type I ELMs transition OS discharges is found to deviate strongly from the known power scaling for this transition, derived for standard H-mode plasmas. In fact, type III ELMs are still observed at much higher power in OS scenarios, and this experimental observation suggests that larger current fraction at the plasma edge in OS discharges , compared to standard H-mode could prevent the type III to I ELMs transition. This observation for OS shear plasmas is attributed to peeling modes instability at the edge, suppresses at lower power in standard H-modes.

1.HIGH TRIANGULARITY PLASMAS.

Results from many divertor tokamaks have shown that high confinement and high density can be achieved simultaneously mainly due to the improved edge stability [1,2,3,4,5] and in particular the access to the second stable regime for ideal ballooning modes at high triangularity [5]. Also core confinement improves with triangularity [1]. Recently, plasmas with high pedestal pressure and small ELMs (Type II [2] or Grassy ELM regimes [4]) have been obtained. These "small ELMs" are characterised by typical MHD edge activity and provide power exhaust through External Transport Barrier (ETB) without significant pedestal pressure degradation, with pedestal energy comparable to that of type I ELMs regime even at high fuelling level. These scenarios are of great interest for the reference ITER ELMy-H mode operation [6] since they potentially provide high confinement at high density and at the same time small energy losses per ELM, that translate in acceptable power density at the divertor target.

1.1 Experimental Observations in ITER-like Configuration in JET.

Recent experiments on plasma shaping effects in JET ELMy H-modes [7] have extended the range of parameters from MkII experiments [1], to *δ~0.47*, near to the values of ITER triangularity. The results of these experiments are summarised in Fig.1, showing the dependence of the

confinement factor H_{97} on the Greenwald number n_e/n_{GR} for gas scans for 2.5MA/2.7T plasmas with δ~*0.47*, and for lower triangularity δ~*0.2-0.3*. The best plasma performances (H_{97}=*0.85* β_N~*1.9,* n_e~*1.1*n_{GR}) were achieved in ITER-like configuration *(*δ~*0.47*) for safety factor q_{95}~*3* where high pedestal pressure and type I ELMs activity is sustained up to the highest density. The anomalous decrease of type I ELMs frequency to the values of unfuelled case *(~12Hz)* was observed at high gas rate *(~4-5.*10^{22}*/s)* at δ~0.47 (Fig.2), but without complete disappearance of type I ELMs, compared to [2,3,4] experiments. Further increase of fuelling *(>6.*10^{22}*/s)* in high triangularity discharges in JET leads to type III ELMs and confinement degradation (Fig.1). Experiments on plasma shaping in other tokamaks reported the improvement of edge stability and hence global plasma performances at high triangularity and rather high value of safety factor (>4.2 in ASDEX-U [2], >6 in JT-60 [4]). Discharges at δ~*0.47* and lower values of plasma current I_p=*2MA (*q_{95}~*4)* and *1.5MA(*q_{95}~*5)* have high ELMs frequency *(* f_{elm}*>60 Hz for* q_{95}~ *4 and* f_{elm} *>100Hz for* q_{95}~*5)* (Fig.2) according to known empirical JET scaling for unfuelled discharges [8] : f_{elm}~*8.9*$P_{sep}/I_p^{1.84}$*(Hz,MW,MA)*, were P_{sep} is power crossing separatrix. The signature of anomalous f_{elm} decrease at high gas level is present at I_p=*2MA* (Fig.2), but at *Ip=1.5MA* rapid increase of f_{elm} with gas fuelling and transition to type III ELMs was observed. High ELM frequency in gas scans at δ~*0.47* and *q95~4; 5* lead to high energy losses in ELMs and plasma performances similar to low triangularity plasmas (Fig.1).

The series of discharges carried out at the reduced vessel wall temperature of T_v=*200°* are characterised by a Type I ELM frequency at medium gas *(~2.*10^{22}*/s)* approximately twice as high as at T_v=*320°* at the same plasma parameters: *~15MW* of NBI, *2.7T/2.5MA*, n_e/n_{GR}~*0.95*. The main chamber recycling level is also approximately twice higher at lower vessel temperature (Fig.3). This observation suggests that not only pedestal parameters but also plasma wall interaction defines the "natural" ELM frequency in the discharge. At the highest gas level, the external fuelling is dominant over the recycling flux and the ELMs behaviour at both temperatures is similar, in particular both exhibit similar anomalous ELMs frequency decrease.

The analysis of the ELM frequency and energy losses for the high δ ELMy H-modes is summarised in figure 4a and 4b, showing the relative diamagnetic energy losses per ELM $\Delta W_{ELM}/W_{tot}$ versus ELM frequency and Greenwald number, averaged over ~10 ELMs. At low density the energy losses per ELM decrease with ELM frequency as usual [9], but for the shots at highest density (~1.1n_{GR}) with anomalous low frequency, the ELMs are relatively small, with $\Delta W_{ELM}/W_{tot}$ ~3% compared to 5-6% for lower density plasmas at the same f_{ELM}. A possible qualitative explanation of the decrease in ELM frequency at high density is the presence of additional losses mechanism in between ELMs. In ITER-like scenarios the broad band 0-30kHz of magnetic fluctuations systematically appears at high density in the discharges with anomalous ELMs frequency (Fig.5). The time-correlation analysis of signals from toroidally separated pick-up coils identifies the main toroidal number to be n=-8. This MHD activity in high density, high triangularity discharges were associated with so-called type II ELMs by analogy with observations

reported by ASDEX-U [2]. There, the type II ELMs regimes provides high pedestal pressure comparable with type I regime and good confinement even at high density, as it was also observed in JET. It's difficult to establish unequivocally if this MHD activity provides any additional electron turbulent transport at the edge, since one measure only fluctuations of poloidal magnetic field dB_θ/dt. In the case of ASDEX-U, this hypothesis is supported by the infrared camera measurements at the divertor target, showing quasi-steady heat flux to the divertor with significantly reduced amplitude during type II ELMs compared to the large heat fluxes during type I ELM [2]. Unfortunately infrared images of the divertor tiles in JET are not available because of the restricted view at high triangularity ~ *0.5*. An interesting feature is that the amplitude of the fast magnetic signal during a type I ELM decreases with density as it shown in Fig.6, which can be related to the fact of decreased energy losses per ELM at highest density in JET (Fig.4b). This explanation doesn't exclude possible role of "plugging effect" of parallel transport to divertor, which limits the energy losses per ELM at high collisionality and hence high density [10].

1.2 Pedestal Stability Analysis.

The ideal ballooning and external low n kink (or peeling) modes are considered for the moment as a most probable candidate for the type I ELMs activity at the edge [11]. Previous calculations of edge stability for low triangularity plasmas *(δ~0.21)* in JET showed that there was no access to the second stability region for the ballooning modes [1]. In this paper, a similar MHD stability analysis was carried out for high-density (~$1.1n_{GR}$) ITER-like triangularity pulse (#52308). Figure 6 shows a comparison between experimental pressure profiles and the modelling with the JETTO code [12]. In JETTO the transport is reduced to neoclassical thermal diffusivity over the width of ETB barrier, so the pressure gradient builds up at the edge up to the ideal ballooning stability limit and then the type I ELM is triggered as a instantaneous increase of heat and particle transport, after that the cycle repeats. JETTO contains an equilibrium module, which calculates the edge magnetic surfaces self-consistently with the edge pressure gradient and bootstrap current in ETB. JETTO pressure and current profiles on the edge magnetic surfaces $0.94<\psi<0.98$ are analysed for ideal ballooning and low n external kink-mode stability by the MISHKA [13] code. From the stability diagram presented in Fig.7 follows that the analysed profiles have possible access to the second stability zone for ballooning modes, while being at the same time stable for n=1 external kink mode, which can explain the high pedestal pressure and good confinement in high triangularity plasmas. The pressure gradient parameter is defined as: $\alpha = -\frac{2\mu_0 q^2}{\varepsilon B_0^2}\frac{dp}{dr}$, where r is the radial co-ordinate of the magnetic surface, B_0-the vacuum magnetic field at the axis, $\varepsilon=a/R$. The edge current is normalized to the current on the analysed magnetic surface. For the moment this results should be considered as preliminary, since only one characteristic pressure profile was analysed and not the whole ELM cycle, so it is not yet clear what mechanism triggers a type I ELMs (that were not totally suppressed in the experiment).

The uncertainties in the experimental pedestal measurements, which provide the initial profiles for JETTO, including the characteristic pedestal width and pressure gradients could also influence the results of JETTO transport modelling and therefore the conclusions of the stability analysis. The simple explanation of ELM disappearance in high triangularity plasmas proposed in [14] can also be used to explain the decrease in ELM frequency at high density. Assuming the heat transport through the ETB is neo-classical [15] and the maximum pressure gradient is limited by ballooning stability limit α_{crit}, the maximum heat flux through the ETB can be estimated as in [14]:

$Q_{\max} \propto -n_{ped}\chi^{i}_{neo}\nabla T_{ped} \propto \frac{n_{ped}^2 q^2 Z_{eff}\sqrt{T_{ped}}}{\Delta B_0^2} \propto \frac{n_{ped}Z_{eff}}{\sqrt{T_{ped}}}\alpha_{crit}$, with n_{ped} and T_{ped} being the density and temperature at the top of the pedestal, Δ the pedestal width. In the second ballooning stable zone, both α_{crit}, and n_{ped} increase, so even neo-classical heat diffusivity is sufficient to justify large losses through ETB, that in turns allow for a steady state to be reached without exceeding ballooning limit, leading either to ELMs disappearance as it in [14] or just to an increase the re-heating time in between ELMs, consistent with the observed decrease of the ELMs frequency at high density. Notice that this simple explanation is alternative or complementary to the one based on the increased MHD activity and hence turbulent transport in type II ELMs regimes proposed in section **1.1** of this paper and in [2]

.

2. OPTIMISED SHEAR (OS) REGIMES.

OS plasmas require different edge conditions compared to ELMy-H modes. In JET in particular, only small type III ELM and low pedestal pressure are compatible with Internal Transport Barrier (ITB) while, on the contrary, type I ELMs usually lead to a collapse of the ITB [16]. A comparative study of type III-I ELMs transition in OS discharges and standard H-modes was carried out, measuring the empirical power threshold of type III to I ELMs transition in standard low triangularity (~0.21). Type I ELMy H-modes were obtained for an input power $P_{typeIII/I} \sim \alpha P_{L/H}$, where $P_{L/H}$ is L/H transition threshold and α~1.8-2, as described in [17]. In contrast, in ITB pulses type III ELMs were observed at up to input powers ~5×$P_{L/H}$ (Fig.8), deviating strongly the empirical power scaling. To compare the physics of the type III to I ELM transition in ITB plasmas to standard ELMy H-modes, the discharge #52498 was run in the same configuration as an OS pulse (#51672) using the same heating scheme. The electron temperature-mapping diagram (time and radius) and D_α signal for the typical OS discharge (#51672) with 12.5MW NBI and 4 MW of ICRH power with ~1.7MW of LHCD pre-heat. The ITB formed at~45.5s and was destroyed by a giant ELM at ~46s. In order to avoid ITB formation in #52498, no LHCD pre-heat was applied and the main heating was started ~6s later, in the current plateau (Fig.10). As a result a standard H-mode with type I ELMs was obtained in #52498. Notice that in both discharges the density increases at the transition from Type III to Type I ELMs because of the growth of the

external barrier (ETB). This experiment raises the question of why in optimised shear discharges type III ELMs are observed for a longer time than in standard H-modes and why sometimes one can produce quasi-stationary (dW/dt=0) high power (~20MW) ITBs during ~10s without a transition to type I ELMs [18]. The hypothesis proposed in this paper is that the type III-I transition is strongly influenced by edge currents, and their effect on stability. In fact, the main feature in an OS scenario compared to H-mode is the different current profile and in particular, OS plasmas have a larger current fraction at the edge. One can use the internal inductance (*li*) and magnetic shear (sh_{95}) to characterise the edge current fraction, since they have lower values for larger pedestal current. Polarimetry measurements at R=3.75m corresponding approximately to the top of the pedestal can also give an indication of the relative current fraction in the pedestal compare to the central plasma. From the polarimetry diagnostic one can estimate $\tilde{B}\big|_{R=3.75m} \sim \int_{-z0}^{z0} B_\theta n dz$, and hence to introduce the parameter $f_j = \frac{\tilde{B}}{I_p \int_{-z0}^{z0} n dz} \sim \frac{I_p - I_{ped}}{I_p}$ proportional to the central current fraction. Here I_p and I_{ped} are total and pedestal currents respectively. The dependence of pedestal density on *li, sh_{95} and f_j* in a series of ITB discharges is shown in Fig.11, suggesting that the transition to high pedestal density and type I ELMs corresponds to the lowest edge current and is correlated to the progressive current diffusion to the centre. Notice that the quasi-stationary long ITB shots with large non-inductive current fraction [18] keep optimised shear current profile and hence high edge current fraction, and indeed the transition to type I ELMs does not occur.

3.CONCLUSIONS AND DISCUSSION.

ITER-like high triangularity *(δ~0.5)* plasmas in JET achieved parameters required for the *Q=10* ITER-FEAT ELMy-H-mode operation [6]: $H_{97}=1$ and $\beta_N \sim 2$ at $n_e/n_{GR}=0.9$ for a safety factor $q_{95} \sim 3$. High pedestal pressure and type I ELMs with reduced frequency *(~12Hz)* and *~3%* energy losses per ELM are sustained up to the highest density *($n_e \sim 1.1 n_{GR}$)*, where an increased broadband MHD activity *(<30kHz, n=-8)* was associated with type II ELMs. The transport and stability analysis with coupled JETTO/MISHKA codes shows possible access to the second stability for ballooning modes and stabilisation of peeling *n=1* mode at high density *($n_e \sim 1.1 n_{GR}$)*.

A Comparative study of type III-I ELMs transition in OS discharges and standard H-modes suggests that the larger edge current fraction in ITB discharges as compared to H-mode can prevent the type III to I ELMs transition. A possible explanation for type I ELMs avoidance in ITB discharges could rely on the presence of the peeling mode instability [10] generated by plasma current in the pedestal region. This hypothesis still requires detailed stability analysis for ITB discharges, which is difficult because of uncertainty in the experimental edge current profile.

REFERENCES

[1] Saibene G. et al., Nuclear Fusion, **39** (1999) 1133.

[2] Stober J. et al., to be published in Nuclear Fusion.

[3] Hubbard A. et al., Phys. of Plasmas, **8** (2001) 2033.

[4] Kamada Y. et al., Plasma Physics Control. Fusion, **42** (2000) A247.

[5] Osborne T.H. et al., Plasma Phys. Control. Fision, **42** (2000) A175.

[6] ITER EDA Doc. Series **N19**, IAEA (2000), I2.3.

[7] Saibene G. et al, 28th EPS, Madeira, Portugal (2001), OT.28.

[8] Kerner W. et al Plasma Physics Control. Fusion, **39**(1997)757.

[9] Horton L.D. et al., Nuclear Fusion, **39** (1999)1.

[10] Loarte A. et al 28th EPS, Madeira, Portugal (2001), P3.005.

[11] Connor J. W. Plasma Phys. Control. Fusion, **40** (1998) 531.

[12] Cherubini A. et al, Plasma Phys. Control. Fusion, **38**(1996)1421.

[13] Huysmans G. T. A.,et al., Nuclear Fusion **38**(1998)179.

[14] Parail V. et al., 28th EPS, Madeira, Portugal (2001), P5.027.

[15] Chang C.S., Hinton F.L. Phys. of Fluids, **29**(1986)3314.

[16] Söldner, F.X. et al. Plasma Phys. Controlled Fusion 39(1997) B353.

[17] Sartori, R., et al, Europhys. Conf. Abstracts **23J**(1999), 197

[18] Litaudon X. et al , 28th EPS, Madeira, Portugal (2001), OT.22.

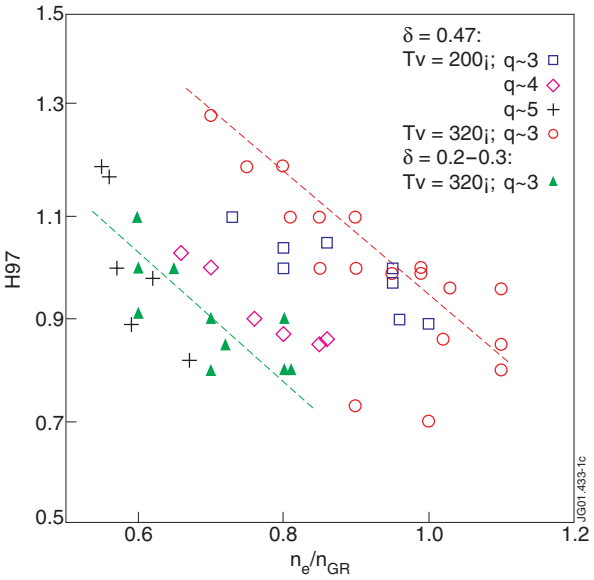

Fig.1: The dependence of confinement factor H_{97} on the Greenwald number n_e/n_{GR} in gas scans for 2.4-2.7T and Ip=2.5,2,1.5MA (q_{95}~3;4;5) in ITER-like configuration (δ~0.47) and in lower triangularity (δ~0.2-0.3) plasmas. At δ~0.47 different vacuum vessel temperatures (T_v=320∞ and T_v=200°) were explored.

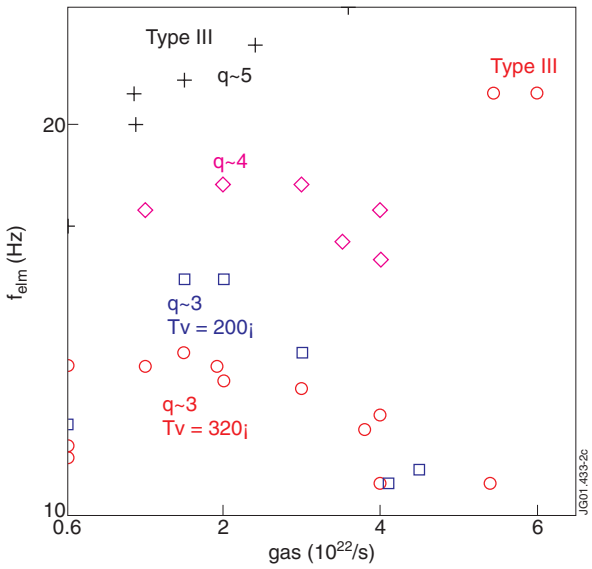

Fig.2: Dependence of ELM frequency at δ~0.47 on the level of D_2 fuelling in the stationary phase for the gas scans presented in Fig.1.

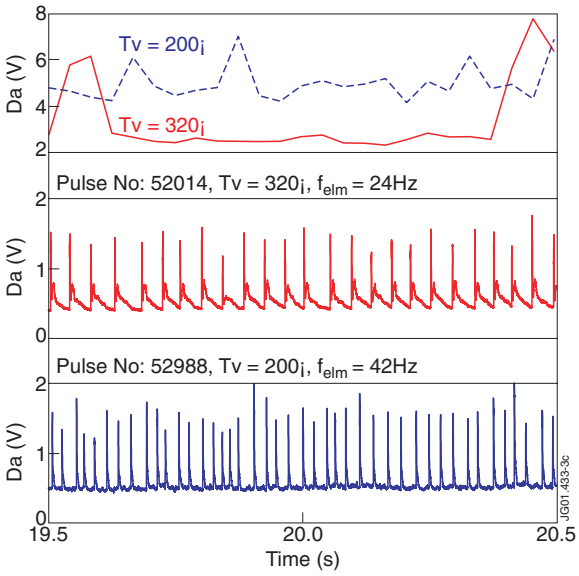

Fig.3: Horizontal D_α photon flux (characteristic of main chamber recycling level) and outer divertor D_α signals for similar discharges at ~15Mw of NBI power, 2.7T/ 2.5MA, n_e/n_{GR}~0.95, D2 fuelling ~2.10^{22}/s at T_v=200°(#52988) and T_v=320° (#52014).

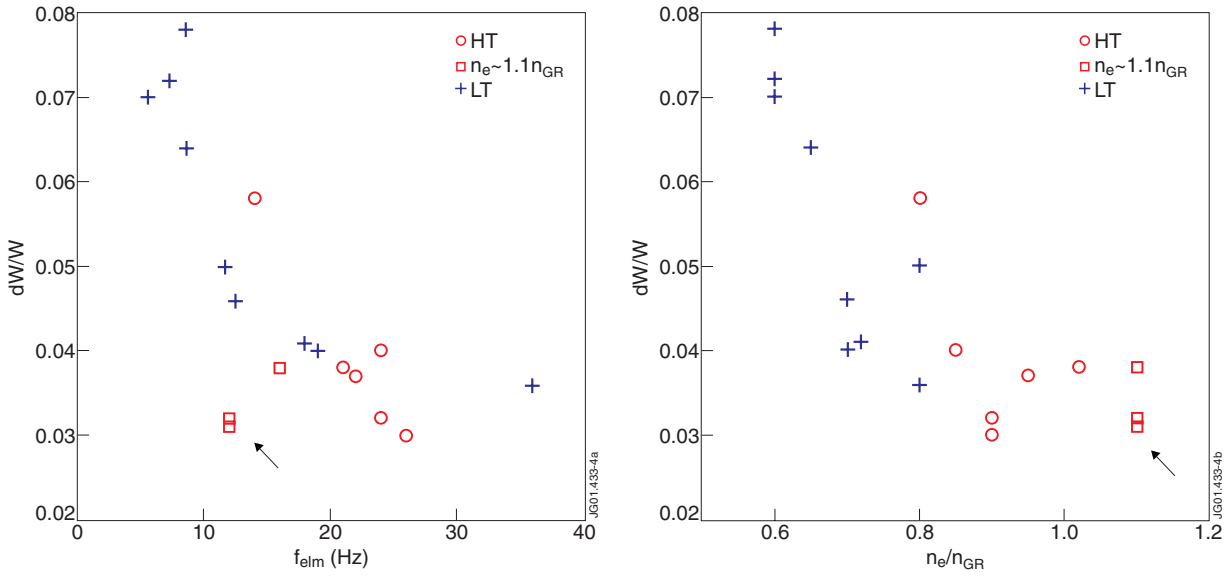

Fig.4: Relative plasma diamagnetic energy losses per ELM (average over~10 ELMs) versus ELM frequency - (a) and Greenwald number (n_e/n_{GR}) - (b) for low triangularity (LT:δ~0.2-0.3) and high triangularity (HT: δ~0.47) plasmas High triangularity high-density n_e/n_{GR}~1.1 pulses are represented by square symbols.

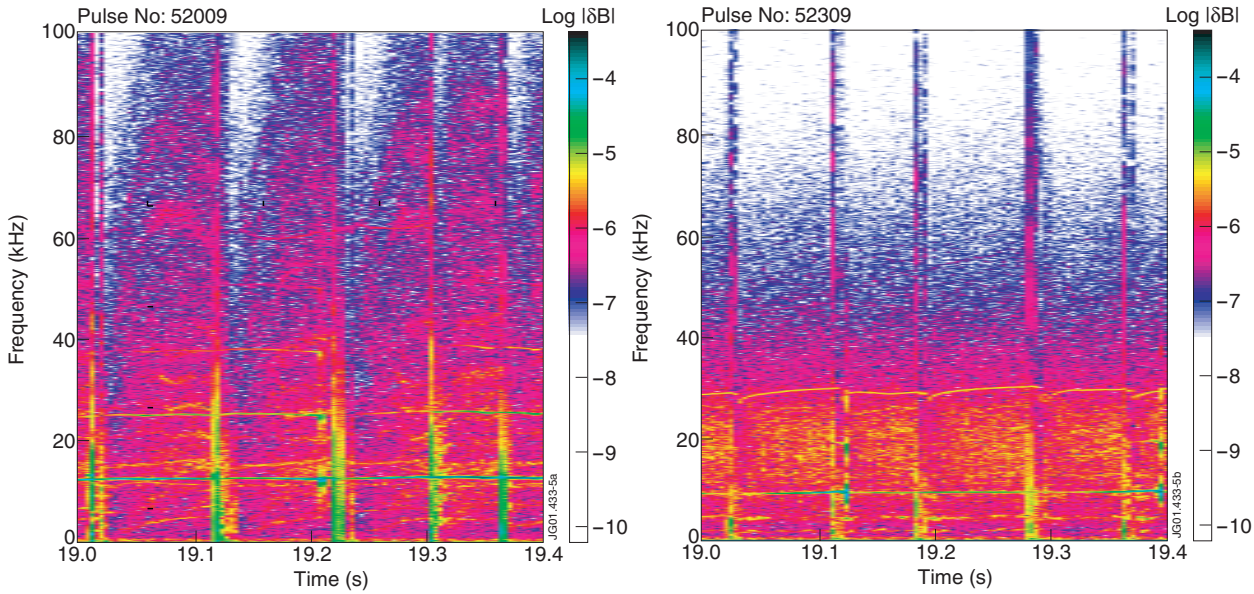

Fig.5: Frequency spectrum of poloidal magnetic perturbation measured by pick-up coils in #52309 (2.7T/2.5MA,δ~0.47, ne/n_{GR}~1.1), where the broadband (<30Hz) MHD activity with n~-8 appears in between type I ELMs (vertical lines in the spectrum).

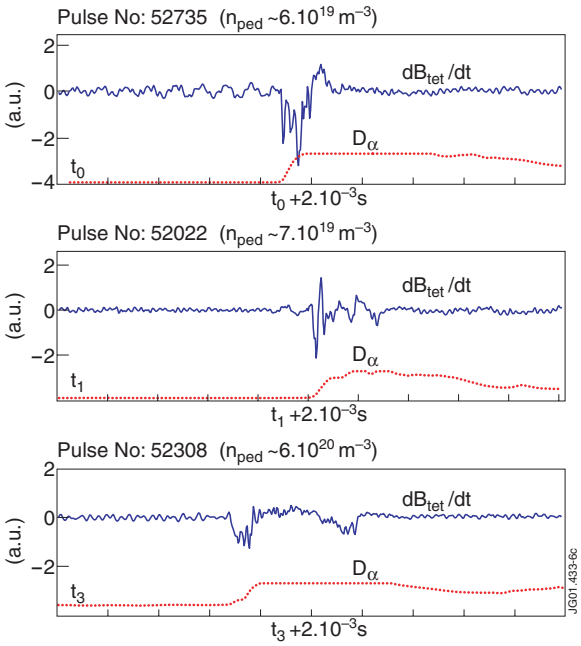

Fig.6: Fluctuations of poloidal magnetic field dB_θ/dt measured by fast Mirnov pick-up coil during an type I ELM in the gas scan for ITER-like high triangularity, 2.7T/2.5MA. The amplitude decreases with increasing pedestal density.

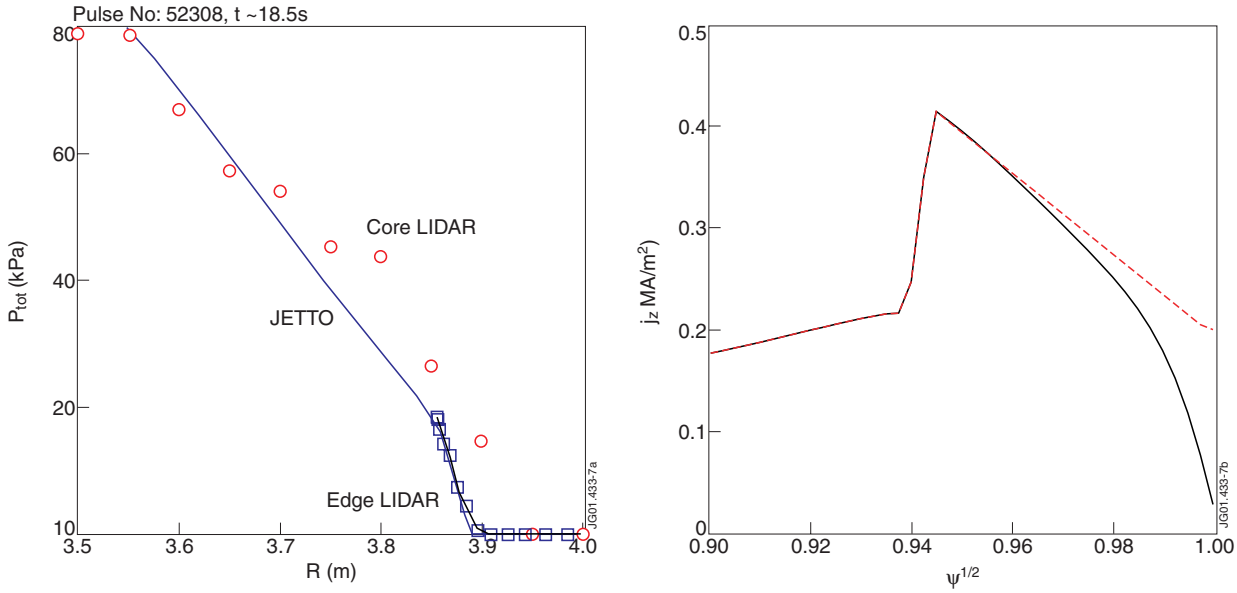

Fig.7: Experimental and modelled by JETTO pressure profiles in JET pulse #52308 (2.7T/2.5MA, δ~0.47, ne/n_{GR}~1.1).

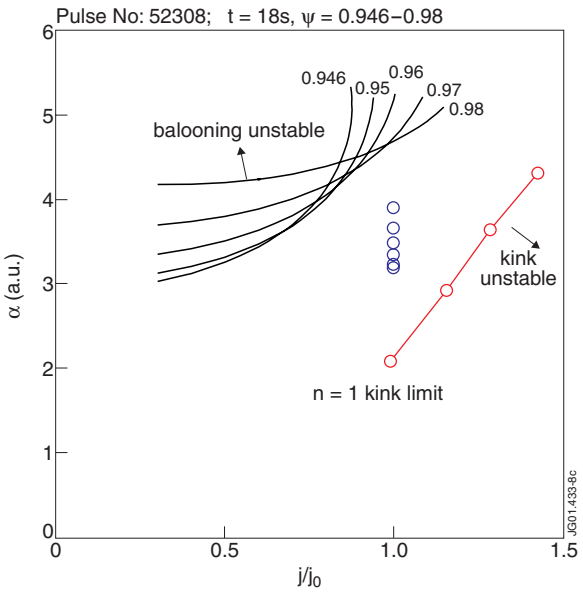

Fig.8: Ballooning mode and external n=1 kink stability diagram calculated by MISHKA for high triangularity (δ~0.47), high density (ne/n_{GR}~1.1) pulse #52308 for the edge magnetic surfaces: 0.94<ψ<0.98.

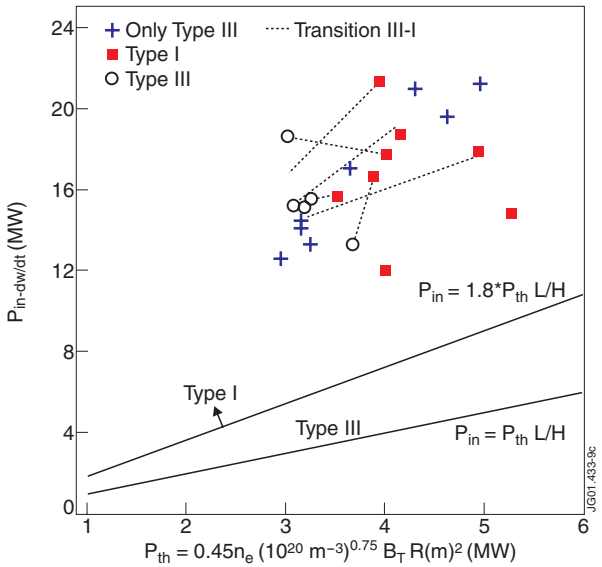

Fig.9: Transition from type III to I ELMs in OS discharges compare to the standard ELMy H-modes. P_{in}- input power in the scaling is replaced by Pin-dW/dt to take into account the non-stationary phase of ITB formation (when time derivation of diamagnetic energy dW/dt>0), $P_{thL/H}$ -L/H transition power threshold, Pin~1.8$P_{thL/H}$ –empirical type III/I transition threshold for standard H-mode from [16].

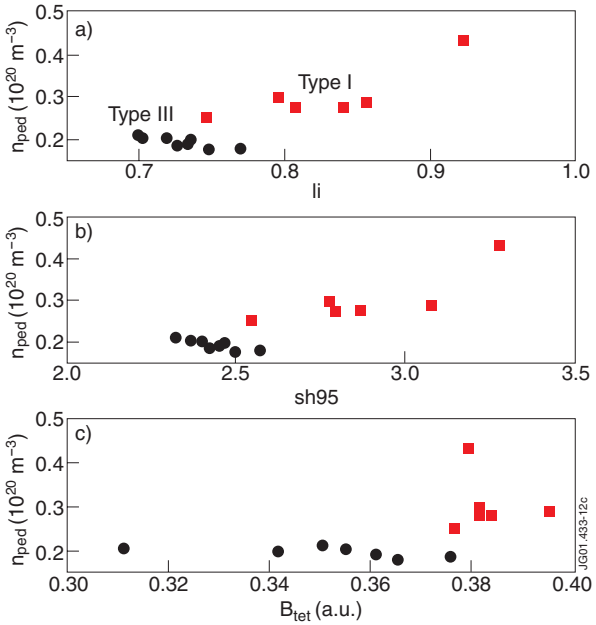

Fig.10: Pedestal density dependence and type III to I ELMs transition in ITB discharges versus internal inductance li- (a), magnetic shear sh_{95}- (b) and central current fraction parameter fj- (c) from polarimetry diagnostic.

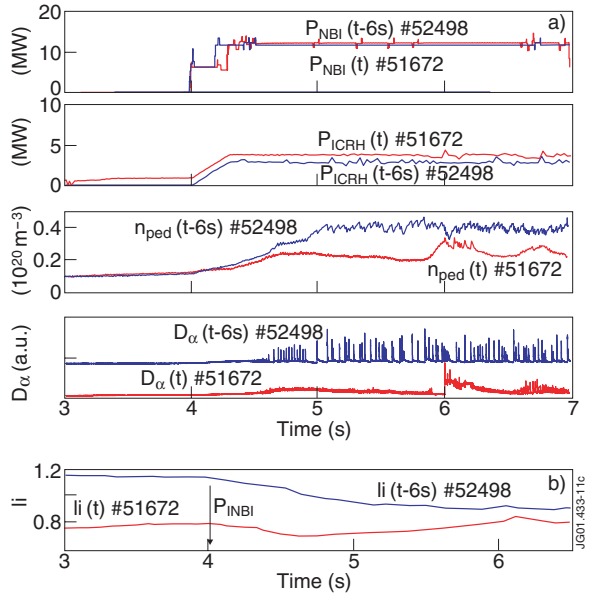

Fig.11: Comparison of standard ELMy H-mode #52498 and OS pulse #51672, run with the same configuration and heating scheme. In order to avoid ITB formation in #52498, LHCD pre-heat was missing and the main heating was applied ~6s latter on the current plateau. Time traces of #52498 are shifted by –6s for comparison with #51672.